

PNEUMATICALLY ACTUATED ACTIVE SUSPENSION SYSTEM FOR REDUCING VEHICLE DIVE AND SQUAT

Fauzi bin Ahmad, Khisbullah Hudha, and Mohd Hanif Bin Harun

Smart Material and Automotive Control (SMAC) Group
Faculty of Mechanical Engineering
Universiti Teknikal Malaysia Melaka (UTeM)
Karung Berkunci 1200, Hang Tuah Jaya, Ayer Keroh 75450 Melaka, Malaysia

ABSTRACT

This manuscript provides a detailed derivation of a full vehicle model, which may be used to simulate the behavior of a vehicle in longitudinal direction. The dynamics of a 14 degrees of freedom (14- DOF) vehicle model is derived and integrated with an analytical tire dynamics namely Calspan tire model. The full vehicle model is then validated experimentally with an instrumented experimental vehicle based on the driver input from brake or throttle. Several transient handling tests are performed, including sudden acceleration test and sudden braking test at constant speed. Comparisons of the experimental result and model response with sudden braking and throttling imposed motion are made. The results of model validation showed that the trends between simulation results and experimental data are almost similar with acceptable error. An active suspension control system is developed on the validated full vehicle model to reduce unwanted vehicle motions during braking and throttling maneuver. A proportional-integral-derivative (PID) scheme integrated with pitch moment rejection loop is proposed to control the system. In presented scheme the result verify improved performance of the proposed control structure during braking and throttling maneuvers compared to the passive vehicle system. It can also be noted that the additional pitch moment rejection loop is able to further improve the performance of the PID controller for the system. The proposed controller will be used to investigate the benefits of a pneumatically actuated active suspension system for reducing unwanted vehicle motion in longitudinal direction.

Keyword: Active suspension, 14 D.O.F. vehicle model, validation, PID, pitch moment rejection.

*Corresponding author : fauzi_ahmad1984@yahoo.com.my

1.0 INTRODUCTION

Vehicle's suspension system is meant to provide safety and comfort for the occupants. Both, vehicle comfort and driving safety are mostly influenced by vertical accelerations and vehicle movements caused by pitch and roll motions [1]. The suspension system perform six basic functions, they are: maintain correct vehicle ride height, reduce the effect of shock forces, maintain correct wheel alignment, support vehicle weight, keep the tires in contact with the road and control the vehicle's direction of travel. Without the suspension system, all of wheel's vertical energy will be transferred to the frame, causing the frame to moves in the same direction with the wheel.

Considering the characteristic of the vehicle movement in longitudinal direction, the vehicle will dive forward when brake is applied. This is due to the fact that, inertia will cause a shift in the vehicle's center of gravity and weight will be transferred from the rear tires to the front tires. Similarly, the vehicle will squat to the rear when throttle input is applied. This is due to the weight transfer from the front to the rear. Both dive and squat are unwanted vehicle motions known as vehicle pitching [1, 2, 3]. This motion will cause instability to the vehicle, lack of handling performance, out of control and moreover may cause an accident [4].

To avoid the unwanted pitching motion, a considerable amount of works have been carried out to solve the problem. Through the combination of mechanical, electrical and hydraulic components, a wide range of controllable suspension systems have been developed varying in cost, sophistication and effectiveness. In general, these systems can be classified into three categories: active suspensions [5, 6] semi-active suspensions [7] and active anti-roll bars [8]. Active suspensions have the ability to add energy into the system, as well as store and dissipate it. A semi active suspension is a passive system with controlled components usually the orifice or the fluid viscosity, which is able to adjust the stiffness of the damper. Whereas the active anti-roll bar system consists of an anti-roll bar mounted in the body and two actuators on each axle to cancel out the unwanted body motion.

In recent years many researches in active suspension have resulted with various control strategies to be developed to cancel out weight transfer using active force control strategy [9], single input rule modules fuzzy reasoning and a disturbance observer [10], integrated control of suspension and steering to [11] and adaptive fuzzy active force control [12]. Other than that, the research on stabilizing body pitch and heave were investigated with various control strategies by Wang and Smith [13]; Labaryade et al. [14], Kruczek et al. [15] and Toshio and Atsushi [16]. Some of the studies used 4-DOF vehicle model [17, 18] 7-DOF vehicle model has been investigated by [19], and [19]

Investigation of active suspension systems for car models is recently increasing much because when compared to passive and semi-active suspension systems, they offer better riding comfort to passengers of high-speed ground transportation. Generally, linear active suspension systems are derived by optimal control theory on the assumption that the car model is described by a linear or approximately linear system whose performance index is given in the quadratic form of the state variables and the [6, 7, 21, 22, 23, 24]. However, nonlinear and

intelligent active suspension systems are proposed for complicated models with no negligibly strong non-linearity and uncertainty. Numerical and experimental results showed that such active suspension systems give relatively more satisfactory performance, but need more increasing loads to achieve active control, compared with the linear active suspension systems [25 - 29]. In this study a pneumatically actuated active suspension (PAAS) for reducing unwanted vehicle motion in longitudinal direction is proposed. The proposed PAAS system is used to minimize the effects of unwanted pitch and vertical body motions of the vehicle in the presence of braking or throttle input from the driver. The aims of using active suspension system are to improve stability, maneuverability and passenger comfort, the active suspension system is the system in which the passive suspension system is augmented by pneumatic actuators that supply additional external forces. The necessary forces for the four unit pneumatic system are determined by a controller using the data from the sensors attached to the vehicle.

The proposed PAAS system is developed using four units pneumatic system installed between lower arms and vehicle body. The proposed control strategy for the PAAS system is the combination of a PID scheme for the feed back control and pitch moment rejection loop for the feed forward control [30 - 33]. Feedback control is used to minimize unwanted body pitch motions, while the feed forward control is intended to reduce the unwanted weight transfer during braking or throttle input maneuvers. The forces produced by the proposed control structure are used as the target forces by the four unit pneumatic system

The proposed control structure is implemented on a validated full vehicle model. The full vehicle model can be approximately described as a 14 DOF system subject to excitation from braking and throttling inputs. It consists of 7-DOF vehicle ride model and 7-DOF vehicle handling model coupled with Calspan tire model [8, 34, 35]. MATLAB-Simulink software is chosen as a computer simulation tool used to simulate the vehicle dynamics behavior and evaluate the performance of the control structure. In order to verify the effectiveness of the proposed controller, passive system and active system with PID controller without pitch moment rejection are selected as the benchmark.

This paper is organized as follows: The first section contains the introduction and the review of some related works, followed by mathematical derivations of 14-DOF full vehicle model with Calspan tire model in the second section. The third section presents the proposed control structure for the pneumatically actuated active suspension system. The following section explains about the validation of 14-DOF vehicle model with the data obtained from instrumented experimental vehicle. The fifth section presents the performance evaluation of the proposed control structure. The last section contains some conclusion.

2.0 FULL VEHICLE MODEL WITH CALSPAN TIRE MODEL

The full-vehicle model of the passenger vehicle considered in this study consists of a single sprung mass (vehicle body) connected to four unsprung masses and is represented as a 14-DOF system. The sprung mass is represented as a plane and is allowed to pitch, roll and yaw as well as to displace in vertical, lateral and longitudinal directions. The unsprung masses are allowed to bounce vertically

with respect to the sprung mass. Each wheel is also allowed to rotate along its axis and only the two front wheels are free to steer.

2.1 Modeling Assumptions

Some of the modeling assumptions considered in this study are as follows: the vehicle body is lumped into a single mass which is referred to as the sprung mass, aerodynamic drag force is ignored, and the roll centre is coincident with the pitch centre and located at just below body center of gravity. The suspensions between the sprung mass and unsprung masses are modeled as passive viscous dampers and spring elements. Rolling resistance due to passive stabilizer bar and body flexibility are neglected. The vehicle remains grounded at all times and the four tires never lost contact with the ground during maneuvering. A 4 degrees tilt angle of the suspension system towards vertical axis is neglected ($\cos 4 = 0.998 \approx 1$). Tire vertical behavior is represented as a linear spring without damping, whereas the lateral and longitudinal behaviors are represented with Calspan model. Steering system is modeled as a constant ratio and the effect of steering inertia is neglected.

2.2 Vehicle Ride Model

The vehicle ride model is represented as a 7-DOF system. It consists of a single sprung mass (car body) connected to four unsprung masses (front-left, front-right, rear-left and rear-right wheels) at each corner. The sprung mass is free to heave, pitch and roll while the unsprung masses are free to bounce vertically with respect to the sprung mass. The suspensions between the sprung mass and unsprung masses are modeled as passive viscous dampers and spring elements. While, the tires are modeled as simple linear springs without damping. For simplicity, all pitch and roll angles are assumed to be small. This similar model was used by Ikenaga [19].

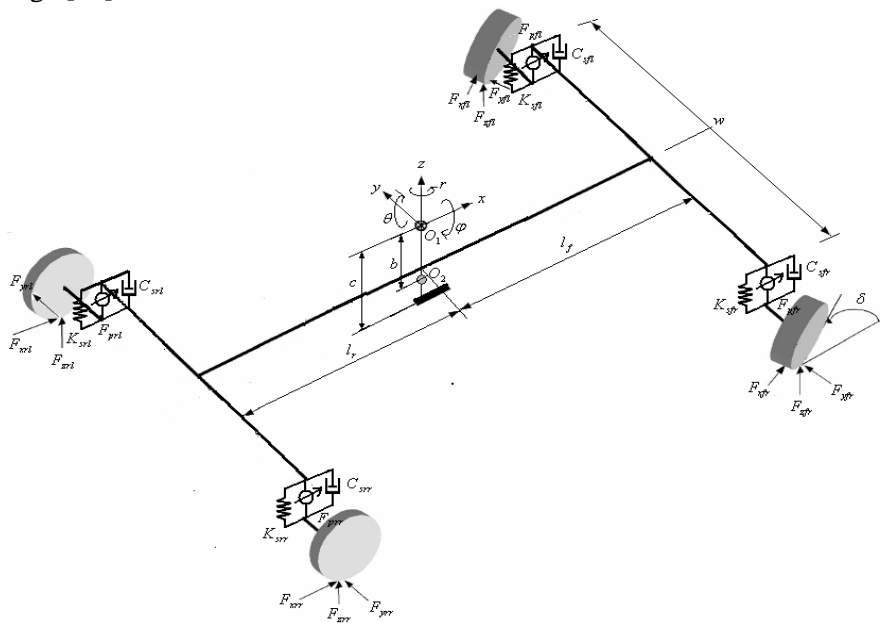


Figure 1: A 14-DOF Full vehicle ride and handling model

Referring to Figure 1, the force balance on sprung mass is given as

$$F_{fl} + F_{fr} + F_{rl} + F_{rr} + F_{pfl} + F_{pfr} + F_{prl} + F_{prr} = m_s \ddot{Z}_s \quad (1)$$

where,

- F_{fl} = suspension force at front left corner
- F_{fr} = suspension force at front right corner
- F_{rl} = suspension force at rear left corner
- F_{rr} = suspension force at rear right corner
- m_s = sprung mass weight
- \ddot{Z}_s = sprung mass acceleration at body centre of gravity

$F_{pfl}; F_{pfr}; F_{prl}; F_{prr}$ = pneumatic actuator forces at front left, front right, rear left and rear right corners, respectively.

The suspension force at each corner of the vehicle is defined as the sum of the forces produced by suspension components namely spring force and damper force as the followings

$$\begin{aligned} F_{fl} &= K_{s,fl}(Z_{u,fl} - Z_{s,fl}) + C_{s,fl}(\dot{Z}_{u,fl} - \dot{Z}_{s,fl}) \\ F_{fr} &= K_{s,fr}(Z_{u,fr} - Z_{s,fr}) + C_{s,fr}(\dot{Z}_{u,fr} - \dot{Z}_{s,fr}) \\ F_{rl} &= K_{s,rl}(Z_{u,rl} - Z_{s,rl}) + C_{s,rl}(\dot{Z}_{u,rl} - \dot{Z}_{s,rl}) \\ F_{rr} &= K_{s,rr}(Z_{u,rr} - Z_{s,rr}) + C_{s,rr}(\dot{Z}_{u,rr} - \dot{Z}_{s,rr}) \end{aligned} \quad (2)$$

where,

- $K_{s,fl}$ = front left suspension spring stiffness
- $K_{s,fr}$ = front right suspension spring stiffness
- $K_{s,rr}$ = rear right suspension spring stiffness
- $K_{s,rl}$ = rear left suspension spring stiffness
- $C_{s,fr}$ = front right suspension damping
- $C_{s,fl}$ = front left suspension damping
- $C_{s,rr}$ = rear right suspension damping
- $C_{s,rl}$ = rear left suspension damping
- $Z_{u,fr}$ = front right unsprung masses displacement
- $Z_{u,fl}$ = front left unsprung masses displacement
- $Z_{u,rr}$ = rear right unsprung masses displacement
- $Z_{u,rl}$ = rear left unsprung masses displacement
- $\dot{Z}_{u,fr}$ = front right unsprung masses velocity
- $\dot{Z}_{u,fl}$ = front left unsprung masses velocity
- $\dot{Z}_{u,rr}$ = rear right unsprung masses velocity

$\dot{Z}_{u,rl}$ = rear left unsprung masses velocity

The sprung mass position at each corner can be expressed in terms of bounce, pitch and roll given by

$$\begin{aligned} Z_{s,fl} &= Z_s - a \sin \theta + 0.5w \sin \varphi \\ Z_{s,fr} &= Z_s - a \sin \theta - 0.5w \sin \varphi \\ Z_{s,rl} &= Z_s + b \sin \theta + 0.5w \sin \varphi \\ Z_{s,rr} &= Z_s + a \sin \theta - 0.5w \sin \varphi \end{aligned} \quad (3)$$

It is assumed that all angles are small, therefore Eq. (3) becomes

$$\begin{aligned} Z_{s,fl} &= Z_s - a\theta + 0.5w\varphi \\ Z_{s,fr} &= Z_s - a\theta - 0.5w\varphi \\ Z_{s,rl} &= Z_s + b\theta + 0.5w\varphi \\ Z_{s,rr} &= Z_s + a\theta - 0.5w\varphi \end{aligned} \quad (4)$$

where,

- a = distance between front of vehicle and C.G. of sprung mass
- b = distance between rear of vehicle and C.G. of sprung mass
- θ = pitch angle at body centre of gravity
- φ = roll angle at body centre of gravity
- $Z_{s,fl}$ = front left sprung mass displacement
- $Z_{s,fr}$ = front right sprung mass displacement
- $Z_{s,rl}$ = rear left sprung mass displacement
- $Z_{s,rr}$ = rear right sprung mass displacement

By substituting Eq. (4) and its derivative (sprung mass velocity at each corner) into Eq. (2) and the resulting equations are then substituted into Eq. (1), the following equation is obtained

$$\begin{aligned} m_s \ddot{Z}_s &= -2(K_{s,f} + K_{s,r})Z_s - 2(C_{s,f} + C_{s,r})\dot{Z}_s + 2(aK_{s,f} - bC_{s,r})\dot{\theta} \\ &+ 2(aC_{s,f} - bC_{s,r})\dot{\varphi} + K_{sf}Z_{u,fl} + C_{s,f}\dot{Z}_{u,fl} + K_{sf}Z_{u,fr} + \\ &+ C_{s,f}\dot{Z}_{u,fr} + K_{sr}Z_{u,rl} + C_{s,r}\dot{Z}_{u,rl} + K_{sr}Z_{u,rr} + C_{s,r}\dot{Z}_{u,rr} \\ &+ F_{pfl} + F_{pfr} + F_{prl} + F_{prr} \end{aligned} \quad (5)$$

where,

- $\dot{\theta}$ = pitch rate at body centre of gravity
- Z_s = sprung mass displacement at body centre of gravity
- \dot{Z}_s = sprung mass velocity at body centre of gravity
- $K_{s,f}$ = spring stiffness of front suspension ($K_{s,fl} = K_{s,fr}$)
- $K_{s,r}$ = spring stiffness of rear suspension ($K_{s,rl} = K_{s,rr}$)

$$\begin{aligned} C_{s,f} &= C_{s,fl} = C_{s,fr} = \text{damping constant of front suspension} \\ C_{s,r} &= C_{s,rl} = C_{s,rr} = \text{damping constant of rear suspension} \end{aligned}$$

Similarly, moment balance equations are derived for pitch θ and roll ϕ , and are given as

$$\begin{aligned} I_{yy} \ddot{\theta} &= 2(aK_{s,f} - bK_{s,r})Z_s + 2(aC_{s,f} - bC_{s,r})\dot{Z}_s - 2(a^2K_{s,f} + b^2K_{s,r})\theta \\ &\quad - 2(a^2C_{s,f} + b^2C_{s,r})\dot{\theta} - aK_{s,f}Z_{u,fl} - aC_{s,f}\dot{Z}_{u,fl} - aK_{s,f}Z_{u,fr} \\ &\quad - aC_{s,f}\dot{Z}_{u,fr} + bK_{s,r}Z_{u,rl} + bC_{s,r}\dot{Z}_{u,rl} + bK_{s,r}Z_{u,rr} + bC_{s,r}\dot{Z}_{u,rr} \\ &\quad - (F_{pfl} + F_{pfr})l_f + (F_{prl} + F_{prr})l_r \end{aligned} \quad (6)$$

$$\begin{aligned} I_{xx} \ddot{\phi} &= -0.5w^2(K_{s,f} + K_{s,r})\phi - 0.5w^2(C_{s,f} + C_{s,r})\dot{\phi} + 0.5wK_{s,f}Z_{u,fl} \\ &\quad + 0.5wC_{s,f}\dot{Z}_{u,fl} - 0.5wK_{s,f}Z_{u,fr} - 0.5wC_{s,f}\dot{Z}_{u,fr} + \\ &\quad + 0.5wK_{s,r}Z_{u,rl} + 0.5wC_{s,r}\dot{Z}_{u,rl} - 0.5wK_{s,r}Z_{u,rr} - 0.5wC_{s,r}\dot{Z}_{u,rr} \\ &\quad + (F_{pfl} + F_{prl})\frac{w}{2} - (F_{pfr} + F_{prr})\frac{w}{2} \end{aligned} \quad (7)$$

where,

$$\begin{aligned} \ddot{\theta} &= \text{pitch acceleration at body centre of gravity} \\ \ddot{\phi} &= \text{roll acceleration at body centre of gravity} \\ I_{xx} &= \text{roll axis moment of inertia} \\ I_{yy} &= \text{pitch axis moment of inertia} \\ w &= \text{wheel base of sprung mass} \end{aligned}$$

By performing force balance analysis at the four wheels, the following equations are obtained

$$\begin{aligned} m_u \ddot{Z}_{u,fl} &= K_{s,f}Z_s + C_{s,f}\dot{Z}_s - aK_{s,f}\theta - aC_{s,f}\dot{\theta} + 0.5wK_{s,f}\phi \\ &\quad + 0.5wC_{s,f}\dot{\phi} - (K_{s,f} + K_t)Z_{u,fl} - C_{s,f}\dot{Z}_{u,fl} + K_tZ_{r,fl} - F_{pfl} \end{aligned} \quad (8)$$

$$\begin{aligned} m_u \ddot{Z}_{u,fr} &= K_{s,f}Z_s + C_{s,f}\dot{Z}_s - aK_{s,f}\theta - aC_{s,f}\dot{\theta} - 0.5wK_{s,f}\phi \\ &\quad - 0.5wC_{s,f}\dot{\phi} - (K_{s,f} + K_t)Z_{u,fr} - C_{s,f}\dot{Z}_{u,fr} + K_tZ_{r,fr} - F_{pfr} \end{aligned} \quad (9)$$

$$\begin{aligned} m_u \ddot{Z}_{u,rl} &= K_{s,r}Z_s + C_{s,r}\dot{Z}_s + bK_{s,r}\theta + bC_{s,r}\dot{\theta} + 0.5wK_{s,r}\phi \\ &\quad + 0.5wC_{s,r}\dot{\phi} - (K_{s,r} + K_t)Z_{u,rl} - C_{s,r}\dot{Z}_{u,rl} + K_tZ_{r,rl} - F_{prl} \end{aligned} \quad (10)$$

$$\begin{aligned} m_u \ddot{Z}_{u,rr} &= K_{s,r}Z_s + C_{s,r}\dot{Z}_s + aK_{s,r}\theta + bC_{s,r}\dot{\theta} - 0.5wK_{s,r}\phi + \\ &\quad - 0.5wC_{s,r}\dot{\phi} - (K_{s,r} + K_t)Z_{u,rr} - C_{s,r}\dot{Z}_{u,rr} + K_tZ_{r,rr} - F_{prr} \end{aligned} \quad (11)$$

where,

$\ddot{Z}_{u,fr}$ = front right unsprung masses acceleration

$\ddot{Z}_{u,fl}$ = front left unsprung masses acceleration

$\ddot{Z}_{u,rr}$ = rear right unsprung masses acceleration

$\ddot{Z}_{u,rl}$ = rear left unsprung masses acceleration

$Z_{r,fr} = Z_{r,fl} = Z_{r,rr} = Z_{r,rl}$ = road profiles at front left, front right, rear right and rear left tires respectively

2.3 Vehicle Handling Model

The handling model employed in this paper is a 7-DOF system as shown in Figure 2. It takes into account three degrees of freedom for the vehicle body in lateral and longitudinal motions as well as yaw motion (r) and one degree of freedom due to the rotational motion of each tire. In vehicle handling model, it is assumed that the vehicle is moving on a flat road. The vehicle experiences motion along the longitudinal x -axis and the lateral y -axis, and the angular motions of yaw around the vertical z -axis. The motion in the horizontal plane can be characterized by the longitudinal and lateral accelerations, denoted by a_x and a_y respectively, and the velocities in longitudinal and lateral direction, denoted by v_x and v_y , respectively.

Acceleration in longitudinal x -axis is defined as

$$\dot{v}_x = a_x + v_y \dot{r} \quad (12)$$

By summing all the forces in x -axis, longitudinal acceleration can be defined as

$$a_x = \frac{F_{xfl} \cos \delta + F_{yfl} \sin \delta + F_{xfr} \cos \delta + F_{yfr} \sin \delta + F_{xrl} + F_{xrr}}{m_t} \quad (13)$$

Similarly, acceleration in lateral y -axis is defined as

$$\dot{v}_y = a_y - v_x \dot{r} \quad (14)$$

By summing all the forces in lateral direction, lateral acceleration can be defined as

$$a_y = \frac{F_{yfl} \cos \delta - F_{xfl} \sin \delta + F_{yfr} \cos \delta - F_{xfr} \sin \delta + F_{yrl} + F_{yrr}}{m_t} \quad (15)$$

where F_{xij} and F_{yij} denote the tire forces in the longitudinal and lateral directions, respectively, with the index (i) indicating front (f) or rear (r) tires and index (j) indicating left (l) or right (r) tires. The steering angle is denoted by δ , the yaw rate by \dot{r} and m_t denotes the total vehicle mass. The longitudinal and lateral vehicle

velocities v_x and v_y can be obtained by the integration of \dot{v}_y and \dot{v}_x . They can be used to obtain the side slip angle, denoted by α . Thus, the slip angle of front and rear tires are found as

$$\alpha_f = \tan^{-1}\left(\frac{v_y + L_f r}{v_x}\right) - \delta_f \quad (16)$$

and

$$\alpha_r = \tan^{-1}\left(\frac{v_y - L_r r}{v_x}\right) \quad (17)$$

Where, α_f and α_r are the side slip angles at front and rear tires respectively. l_f and l_r are the distance between front and rear tire to the body center of gravity respectively.

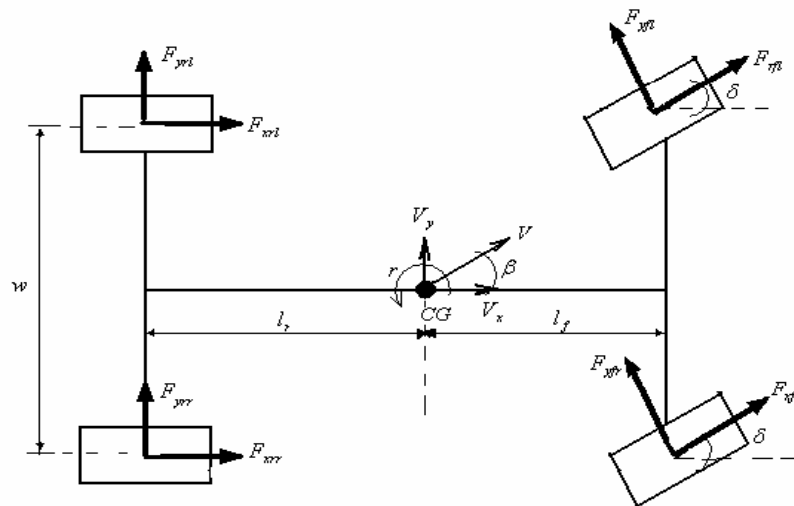


Figure 2: A 7-DOF Vehicle handling model

To calculate the longitudinal slip, longitudinal component of the tire velocity should be derived. The front and rear longitudinal velocity component is given by:

$$v_{wxf} = V_{tf} \cos \alpha_f \quad (18)$$

Where, the speed of the front tire is,

$$V_{tf} = \sqrt{(v_y + L_f r)^2 + v_x^2} \quad (19)$$

The rear longitudinal velocity component is,

$$v_{wxr} = V_{tr} \cos \alpha_r \quad (20)$$

Where, the speed of the rear tire is,

$$V_{tr} = \sqrt{(v_y + L_r r)^2 + v_x^2} \quad (21)$$

Then, the longitudinal slip ratio of front tire,

$$S_{af} = \frac{v_{wxf} - \omega_f R_w}{v_{wxf}} \text{ under braking conditions} \quad (22)$$

The longitudinal slip ratio of rear tire is,

$$S_{ar} = \frac{v_{wxr} - \omega_r R_w}{v_{wxr}} \text{ under braking conditions} \quad (23)$$

where, ω_r and ω_f are angular velocities of rear and front tires, respectively and R_w , is the wheel radius. The yaw motion is also dependent on the tire forces F_{xij} and F_{yij} as well as on the self-aligning moments, denoted by M_{zij} acting on each tire:

$$\ddot{r} = \frac{1}{J_z} \left(\begin{aligned} & \frac{w}{2} F_{xfl} \cos \delta - \frac{w}{2} F_{xfr} \cos \delta + \frac{w}{2} F_{xrl} - \frac{w}{2} F_{xrr} + \frac{w}{2} F_{yfl} \sin \delta - \\ & \frac{w}{2} F_{yfr} \sin \delta - l_r F_{yrl} - l_r F_{yrr} + l_f F_{yfl} \cos \delta + l_f F_{yfr} \cos \delta - l_f F_{xfl} \sin \delta - \\ & l_f F_{xfr} \sin \delta + M_{zfl} + M_{zfr} + M_{zrl} + M_{zrr} \end{aligned} \right) \quad (24)$$

Where, J_z is the moment of inertia around the z-axis. The roll and pitch motion depend very much on the longitudinal and lateral accelerations. Since only the vehicle body undergoes roll and pitch, the sprung mass, denoted by m_s has to be considered in determining the effects of handling on pitch and roll motions as the following:

$$\ddot{\phi} = \frac{-m_s c a_y + \phi(m_s g c - k_\phi) + \dot{\phi}(-\beta_\phi)}{J_{sx}} \quad (25)$$

$$\ddot{\theta} = \frac{-m_s c a_y + \theta(m_s g c - k_\theta) + \dot{\theta}(-\beta_\theta)}{J_{sy}} \quad (26)$$

Where, c is the height of the sprung mass center of gravity to the ground, g is the gravitational acceleration and k_ϕ , β_ϕ , k_θ and β_θ are the damping and stiffness constant for roll and pitch, respectively. The moments of inertia of the sprung mass around x-axes and y-axes are denoted by J_{sx} and J_{sy} respectively.

2.4 Braking and Throttling Torques

For the front and rear wheels, the sum of the torque about the axis as shown in Figure 3 are as follows:

$$F_{xf} R_{\omega} - T_{bf} + T_{af} = I_{\omega} \dot{\omega}_f \quad (27)$$

$$F_{xr} R_{\omega} - T_{br} + T_{ar} = I_{\omega} \dot{\omega}_r \quad (28)$$

Where ω_f and ω_r are the angular velocity of the front and rear wheels, I_{ω} is the inertia of the wheel about the axle, R_{ω} is the wheel radius, T_{bf} and T_{br} are the applied braking torques, and T_{af} and T_{ar} are the applied throttling torques for the front and rear wheels

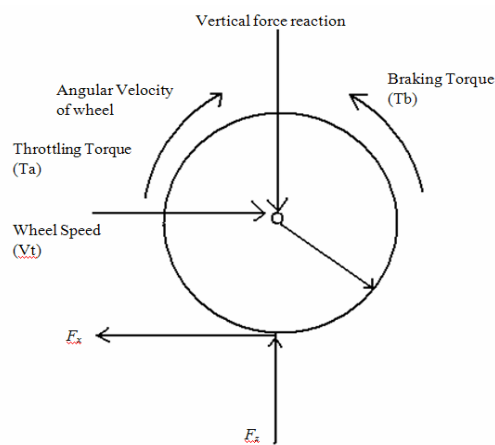


Figure 3: Free Body Diagram of a Wheel

2.5 Simplified Calspan Tire Model

Tire model considered in this study is Calspan model as described in Szostak *et al.* [36]. Calspan model is able to describe the behavior of a vehicle in any driving conditions which may require severe steering, braking, acceleration, and other driving related operations[34]. The longitudinal and lateral forces generated by a tire are a function of the slip angle and longitudinal slip of the tire relative to the road. The previous theoretical developments in Szostak *et al.* [36] lead to a complex, highly non-linear composite force as a function of composite slip. It is convenient to define a saturation function, $f(\sigma)$, to obtain a composite force with any normal load and coefficient of friction values [37]. The polynomial expression of the saturation function is presented by:

$$f(\sigma) = \frac{F_c}{\mu F_z} = \frac{C_1 \sigma^3 + C_2 \sigma^2 + (\frac{4}{\pi}) \sigma}{C_1 \sigma^3 + C_2 \sigma^2 + C_4 \sigma + 1} \quad (29)$$

Where, C_1 , C_2 , C_3 and C_4 are constant parameters fixed to the specific tires. The tire contact patch lengths are calculated using the following two equations:

$$ap_0 = \frac{0.0768 \sqrt{F_z F_{ZT}}}{T_w (T_p + 5)} \quad (30)$$

$$ap = \left(1 - \frac{K_a F_x}{F_z} \right) \quad (31)$$

Where ap is the tire contact patch, T_w is a tread width, and T_p is a tire pressure. The values of F_{ZT} and K_a are tire contact patch constants. The lateral and longitudinal stiffness coefficients (K_s and K_c , respectively) are a function of tire contact patch length and normal load of the tire as expressed as follows:

$$K_s = \frac{2}{ap_0^2} \left(A_0 + A_1 F_z - \frac{A_1 F_z^2}{A_2} \right) \quad (32)$$

$$K_c = \frac{2}{ap_0^2} F_z (CS / FZ) \quad (33)$$

Where the values of A_0 , A_1 , A_2 and CS/FZ are stiffness constants. Then, the composite slip calculation becomes:

$$\sigma = \frac{\pi ap^2}{8\mu_0 F_z} \sqrt{K_s^2 \tan^2 \alpha + K_c^2 \left(\frac{s}{1-s} \right)^2} \quad (34)$$

μ_0 is a nominal coefficient of friction and has a value of 0.85 for normal road conditions, 0.3 for wet road conditions, and 0.1 for icy road conditions. Given the polynomial saturation function, lateral and longitudinal stiffness, the normalized lateral and longitudinal forces are derived by resolving the composite force into the side slip angle and longitudinal slip ratio components:

$$\frac{F_y}{\mu F_z} = \frac{f(\sigma) K_s \tan \alpha}{\sqrt{K_s^2 \tan^2 \alpha + K_c'^2 S^2}} + Y_\gamma \gamma \quad (35)$$

$$\frac{F_x}{\mu F_z} = \frac{f(\sigma) K_c' S}{\sqrt{K_s^2 \tan^2 \alpha + K_c'^2 S^2}} \quad (36)$$

Lateral force has an additional component due to the tire camber angle, γ , which is modeled as a linear effect. Under significant maneuvering conditions with large lateral and longitudinal slip, the force converges to a common sliding friction value. In order to meet this criterion, the longitudinal stiffness coefficient is modified at high slips to transition to lateral stiffness coefficient as well as the coefficient of friction defined by the parameter K_μ .

$$K_c' = K_c + (K_s - K_c) \sqrt{\sin^2 \alpha + S^2 \cos^2 \alpha} \quad (37)$$

$$\mu = \mu_0 (1 - K_\mu) \sqrt{\sin^2 \alpha + S^2 \cos^2 \alpha} \quad (38)$$

2.6 Description of the simulation model

The vehicle dynamics model is developed based on the mathematical equations from the previous vehicle handling equations by using MATLAB-Simulink software. The relationship between handling model, ride model, tire model, slip angle and longitudinal slip are clearly described in Figure 4. In this model there are two inputs that can be used in the dynamic analysis of the vehicle namely torque input and steering input which come from driver. It simply explains that the model created is able to perform the analysis for longitudinal and lateral direction.

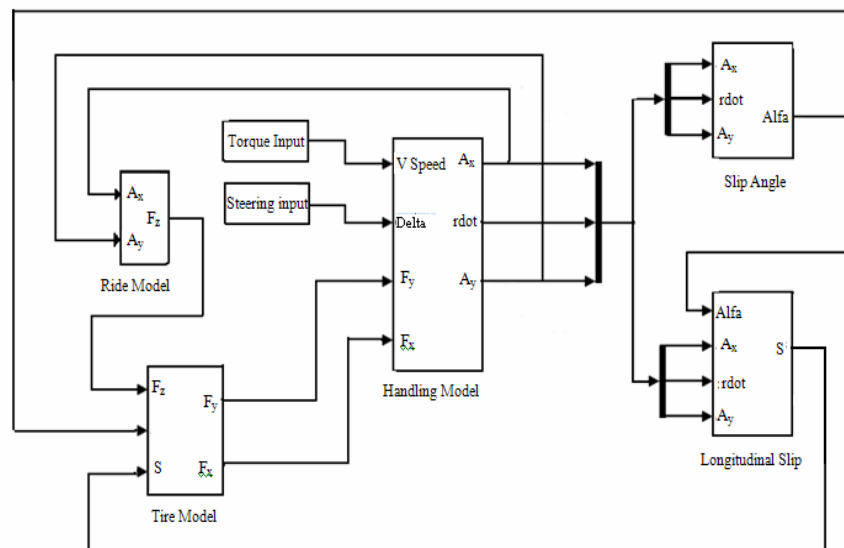


Figure 4: Full Vehicle Model in Matlab-Simulink

3.0 ACTIVE CONTROL SYSTEM DESIGN

The controller structure consists of inner loop controller to reject the unwanted weight transfer and outer loop controller to stabilize heave and pitch responses due to pitch torque input from the driver. An input decoupling transformation is placed between inner and outer loop controllers that blend the inner loop and outer loop controllers. The outer loop controller provides the ride control that isolates the vehicle body from vertical and rotational vibrations induced by pitch torque input. The inner loop controller provides the weight transfer rejection control that maintains load-leveling and load distribution during vehicle maneuvers. The proposed control structure is shown in Figure 5.

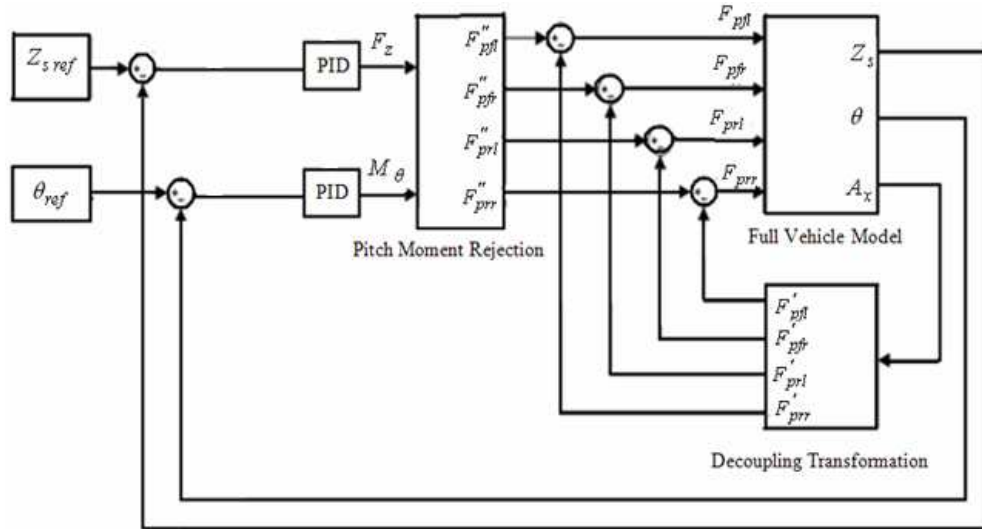


Figure 5: The Proposed Control Structure for Active Suspension System

In this study the PID controller is used in the outer loop control to isolate the vehicle body from vertical and rotational vibrations induced by brake or throttle torque input. The outputs of the outer loop controller are vertical forces to stabilize body bounce (F_z) and moment to stabilize body pitch (M_θ). The PID controller that is applied in the system is shown in Figure 1 and mathematically can be described by equation (39).

$$F_z(t) = k_p(t) e(t) + k_i(t) \int e(t) dt + k_d(t) \frac{d}{dt} e(t) \quad (39)$$

Where $e(t) = Z_s ref(t) - Z_s(t)$ and the proportional gain, $k_p(t)$, integral gain, $k_i(t)$ and derivative gain, $k_d(t)$ are the function of the position error body displacement.

$$M_\theta(t) = k_p(t) e(t) + k_i(t) \int e(t) dt + k_d(t) \frac{d}{dt} e(t) \quad (40)$$

Where $e(t) = \theta_{ref}(t) - \theta(t)$ and the proportional gain, $k_p(t)$, integral gain, $k_i(t)$ and derivative gain, $k_d(t)$ are the function of the position error pitch angle.

3.1 Decoupling Transformation

As mention in Section 3.0 the outputs of the outer loop controller are vertical forces to stabilize body bounce (F_z) and moment to stabilize pitch (M_θ). These forces and moments are then distributed into target forces of the four pneumatic actuators produced by the outer loop controller. Distribution of the forces and moments into target forces of the four pneumatic actuators is performed using decoupling transformation subsystem. The outputs of the decoupling transformation subsystem namely the target forces for the four pneumatic actuators are then subtracted with the relevant outputs from the inner loop

controller to produce the ideal target forces for the four pneumatic actuators. Decoupling transformation subsystem requires an understanding of the system dynamics in the previous section. From equations (5), (6) and (7), equivalent forces and moments for heave, pitch and roll can be defined by:

$$F_z = F_{pfl}'' + F_{pfr}'' + F_{prl}'' + F_{prr}'' \quad (41)$$

$$M_\theta = -F_{pfl}'' l_f - F_{pfr}'' l_f + F_{prl}'' l_r + F_{prr}'' l_r \quad (42)$$

$$M_\varphi = F_{pfl}'' \left(\frac{w}{2} \right) - F_{pfr}'' \left(\frac{w}{2} \right) + F_{prl}'' \left(\frac{w}{2} \right) - F_{prr}'' \left(\frac{w}{2} \right) \quad (43)$$

Where F_{pfl}'' , F_{pfr}'' , F_{prl}'' and F_{prr}'' are the pneumatic forces which are produced by outer loop controller in front left, front right, rear left and rear right corners, respectively. In the case of the vehicle input comes from brake torque, the roll moment can be neglected. Equations (41), (42) and (43) can be rearranged in a matrix format as the following:

$$\begin{bmatrix} f_z(t) \\ M_\theta(t) \\ M_\varphi(t) \end{bmatrix} = \begin{bmatrix} 1 & 1 & 1 & 1 \\ -L_f & -L_f & L_r & L_r \\ \frac{w}{2} & -\frac{w}{2} & \frac{w}{2} & -\frac{w}{2} \end{bmatrix} \begin{bmatrix} F_{pfl}'' \\ F_{pfr}'' \\ F_{prl}'' \\ F_{prr}'' \end{bmatrix} \quad (44)$$

For a linear system of equations $y=Cx$, if $C \in \mathfrak{R}^{m \times n}$ has full row rank, then there exists a right inverse C^{-1} such that $C^{-1}C = I^{m \times m}$. The right inverse can be computed using $C^{-1} = C^T (CC^T)^{-1}$. Thus, the inverse relationship of equation (42) can be expressed as

$$\begin{bmatrix} F_{pfl}'' \\ F_{pfr}'' \\ F_{prl}'' \\ F_{prr}'' \end{bmatrix} = \begin{bmatrix} \frac{l_r}{2(l_f + l_r)} & -\frac{1}{2(l_f + l_r)} & \frac{1}{2w} \\ \frac{l_r}{2(l_f + l_r)} & -\frac{1}{2(l_f + l_r)} & -\frac{1}{2w} \\ \frac{l_f}{2(l_f + l_r)} & \frac{1}{2(l_f + l_r)} & \frac{1}{2w} \\ \frac{l_f}{2(l_f + l_r)} & \frac{1}{2(l_f + l_r)} & -\frac{1}{2w} \end{bmatrix} \begin{bmatrix} F_z \\ M_\theta \\ M_\varphi \end{bmatrix} \quad (45)$$

3.2 Pitch Moment Rejection Loop

In the outer loop controller, PID control is applied for suppressing both body vertical displacement and body pitch angle. The inner loop controller of pitch moment rejection control is described as follows: during throttling and braking, a

vehicle will produce a force namely throttling force and braking force at the body center of gravity respectively. The throttling force generates pitch moment to the pitch pole causing the body center of gravity to shift backward as shown in Figure 6 and vice versa when braking input is applied. Shifting the body center of gravity causes a weight transfer from axle to the other axle. By defining the distance between the body center of gravity and the pitch pole is H_{pc} , pitch moment is defined by:

$$M_p = M(a_x)H_{pc} \quad (46)$$

In case of brake, the two pneumatic actuators installed in the front axle have to produce the necessary forces to cancel out the unwanted pitch moments, whereas the forces of the two pneumatic actuators at the rear axle will act in the opposite from the front pneumatic actuator. Pneumatic forces that cancel out pitch moment in each corner due to braking input are defined as:

$$F'_{pfr} = F'_{pfl} = \frac{M_p(a_x)H_{pc}}{L_f} \text{ and } F'_{prl} = F'_{prr} = -\left(\frac{M_p(a_x)H_{pc}}{L_f}\right) \quad (47)$$

Whereas, pneumatic forces to cancel out pitch moment in each corner for throttle input can be defined as:

$$F'_{prl} = F'_{prr} = \frac{M_p(a_x)H_{pc}}{L_r} \text{ and } F'_{pfl} = F'_{pfr} = -\left(\frac{M_p(a_x)H_{pc}}{L_r}\right) \quad (48)$$

Where,

F_{pfl} = target force of pneumatic system at front left corner produced by inner loop controller

F_{pfr} = target force of pneumatic system at front right corner produced by inner loop controller

F_{prl} = target force of pneumatic system at rear left corner produced by inner loop controller

F_{prr} = target force of pneumatic system at rear right corner produced by inner loop controller

The ideal target forces for each pneumatic actuator are defined as the target forces produced by outer loop controller subtracted with the respective target forces produced by inner loop controller as the following:

$$F_{pfl} = F''_{pfl} - F'_{pfl} \quad (49)$$

$$F_{pfr} = F_{pfr}'' - F_{pfr}' \quad (50)$$

$$F_{prl} = F_{prl}'' - F_{prl}' \quad (51)$$

$$F_{prr} = F_{prr}'' - F_{prr}' \quad (52)$$

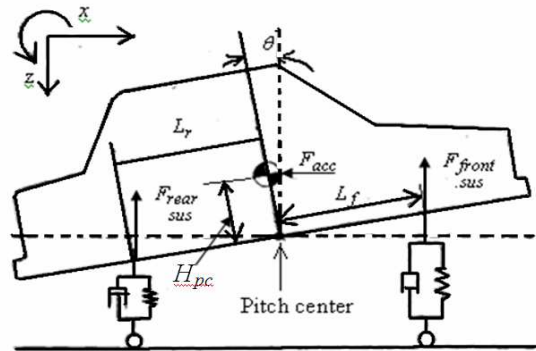


Figure 6: Free body diagram for pitch motion.

4.0 VALIDATION OF 14-DOF VEHICLE MODEL USING INSTRUMENTED EXPERIMENTAL VEHICLE

To verify the full vehicle ride and handling model that have been derived, experimental works are performed using an instrumented experimental vehicle. This section provides the verification of ride and handling model using visual technique by simply comparing the trend of simulation results with experimental data using the same input signals. Validation or verification is defined as the comparison of model's performance with the real system. Therefore, the validation does not mean the fitting of simulated data exactly to the measured data, but as gaining confidence that the vehicle handling simulation is giving insight into the behavior of the simulated vehicle reference. The tests data are also used to check whether the input parameters for the vehicle model are reasonable. In general, model validation can be defined as determining the acceptability of a model by using some statistical tests for deviance measures or subjectively using visual techniques reference.

4.1 Vehicle Instrumentation

The data acquisition system (DAS) is installed into the experimental vehicle to obtain the real vehicle reaction as to evaluate the vehicle's performance in terms of longitudinal acceleration, body vertical acceleration and pitch rate. The DAS uses several types of transducers such as single axis accelerometer to measure the sprung mass and unsprung mass accelerations for each corner, tri-axial

accelerometer to measure longitudinal, vertical and lateral accelerations at the body center of gravity, tri-axial gyroscopes for the pitch rate and wheel speed sensor to measure angular velocity of the tire. The multi-channel μ -MUSYCS system Integrated Measurement and Control (IMC) is used as the DAS system. Online FAMOS software as the real time data processing and display function is used to ease the data collection. The installation of the DAS and sensors to the experimental vehicle can be seen in Figure 7.



Figure 7: In-vehicle instrumentations

4.2 Experimental Vehicle

An instrumented experimental vehicle is developed to validate the full vehicle model. A Malaysian National car is used to perform sudden braking and sudden acceleration test. The tests were partly adopted from SAE J1666, (2002) procedures. Note that the vehicle is 1300 cc and used manual gear shift as the power terrain systems. The technical specifications of the vehicle are listed in Table 1.

4.3 Validation Procedures

The dynamic response characteristics of a vehicle model that include longitudinal acceleration, longitudinal slip in each tire and pitch rate can be validated using experimental test through several handling test procedures namely sudden braking test and sudden acceleration test. Sudden braking test is intended to study transient response of the vehicle under braking input. In this case, the tests were conducted by accelerating the vehicle to a nominal speed of 60kph and activating the instrumentation package. The driver then applies the brake pedal hard enough to hold the pedal firmly until the vehicle stopped completely. On the other hand, sudden acceleration test is used to evaluate the characteristics of the vehicle during a sudden increase of speed. In this study, the vehicle accelerated to a nominal

speed of 40kph and activated the instrument package. The driver then manually applied the throttle pedal full step as required to make the vehicle accelerated immediately.

Table 1: Experimental vehicle Parameter

Parameter	Value
Vehicle mass	920kg
Wheel base	2380mm
Wheel track	1340mm
Spring rate: Front: Rear:	30 N/mm 30 N/mm
Damper rate : Front: Rear:	1000 N/msec ⁻¹ 1000 N/msec ⁻¹
Roll center	100
Center of gravity	550mm
Wheel radius	285mm

4.4 Validation Results

Figures 8 and 9 show a comparison of the results obtained using SIMULINK and experimental. In experimental works, all the experimental data are filtered to remove out any unintended data. It is necessary to note that the measured vehicle speed from the speed sensor is used as the input of simulation model. For the simulation model, tire parameters are obtained from Szostak *et al.* [36] and Singh *et al.* [37]. The results of model verification for sudden braking test at 60 kph are shown in Figure 9. Figure 9(a) shows the vehicle speed applied for the test. It can be seen that the trends between simulation results and experimental data are almost similar with acceptable error. The small difference in magnitude between simulation and experimental results is due to the fact that, in an actual situation, it is indeed very hard for the driver to maintain the in a perfect speed as compared to the result obtained in the simulation.

In terms of both longitudinal acceleration and pitch rate response, it can be seen that there are quite good comparisons during the initial transient phase as well as during the following steady state phase as shown in Figures 8(b) and (c) respectively. Longitudinal slip responses of the front tires also show satisfactory matching with only small deviation in the transition area between transient and steady state phases as shown in Figure 8(d) and (e). It can also be noted that the longitudinal slip responses of all tires in the experimental data are slightly higher than the longitudinal slip data obtained from the simulation responses particularly for the rear tires as can be seen in Figures 8(f) and (g). This is due to the fact that it is difficult for the driver to maintain a constant speed during maneuvering. In simulation, it is also assumed that the vehicle is moving on a flat road during step steer maneuver. In fact, it is observed that the road profiles of test field consist of irregular surface. This can be another source of deviation on longitudinal slip response of the tires.

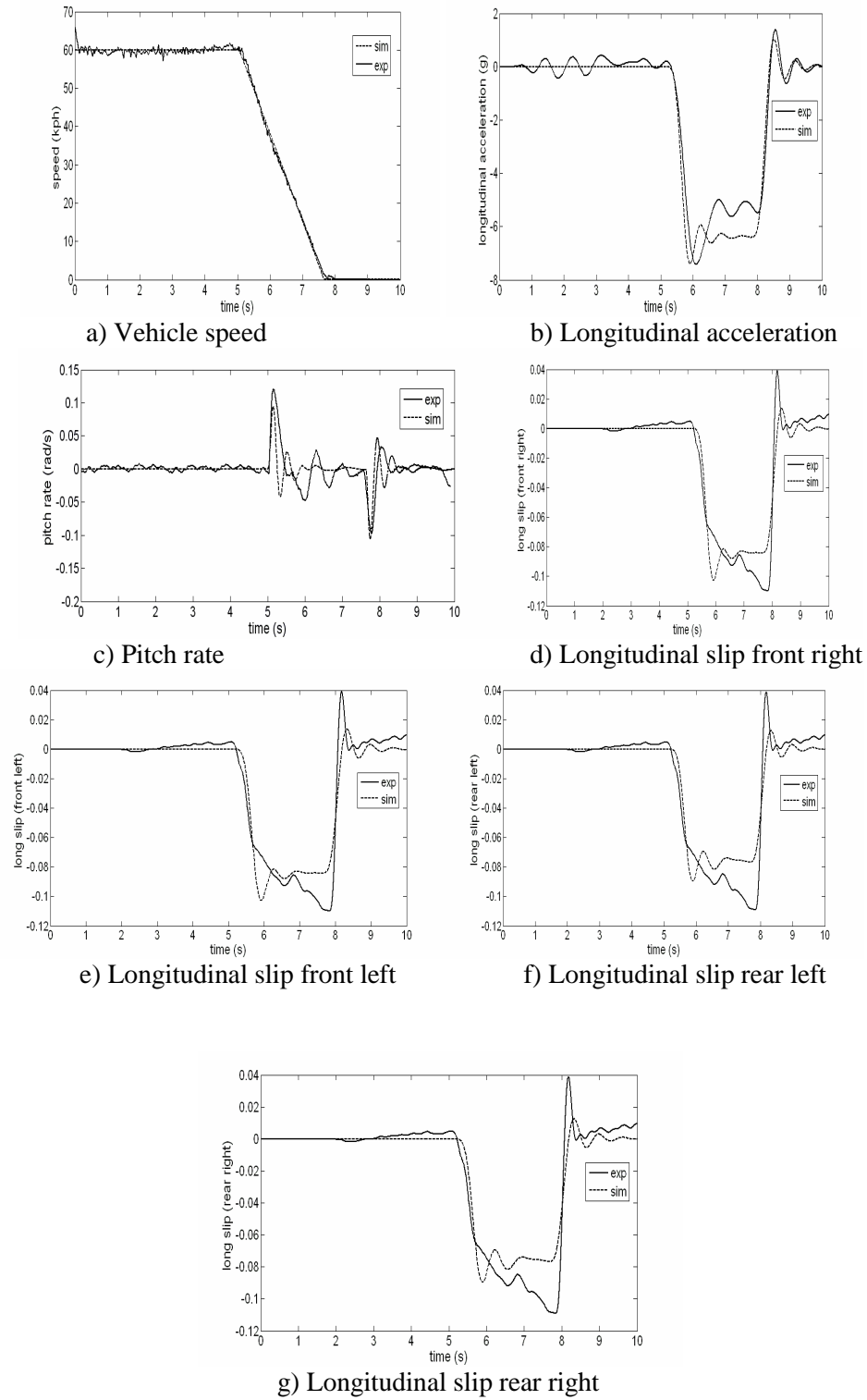


Figure 8: Response of the Vehicle for sudden braking test at 60kph constant

speed.

The results of Sudden Acceleration test at constant speed of 40kph indicate that measurement data and the simulation results agree with a relatively good accuracy as shown in Figure 9. Figure 9(a) shows the vehicle speed which is used as the input for the simulation model. In terms of pitch rate and longitudinal acceleration, it can be seen clearly that the simulation and experimental result are very similar with minor difference in magnitude as shown in Figure 9 (b) and (c). The minor difference in magnitude and small fluctuation occurred on the measured data is due to the body flexibility which was ignored in the simulation model. In terms of tire longitudinal slip, the trends of simulation results show close agreement for both experimental data and simulation and shown in Figure 9(d), (e), (f) and (g). Closely similar to the validation results obtained from sudden acceleration test, the longitudinal slip responses of all tires in experimental data are smaller than the longitudinal slip data obtained from the simulation. Again, this is due to the difficulty of the driver to maintain a constant speed during sudden acceleration test maneuver. Assumption in simulation model that the vehicle is moving on a flat road during the maneuver is also very difficult to realize in practice. In fact, road irregularities of the test field may cause the change in tire properties during vehicle handling test. Assumption of neglecting steering inertia may possibility in lower down the magnitude of tire longitudinal slip in simulation results compared with the measured data.

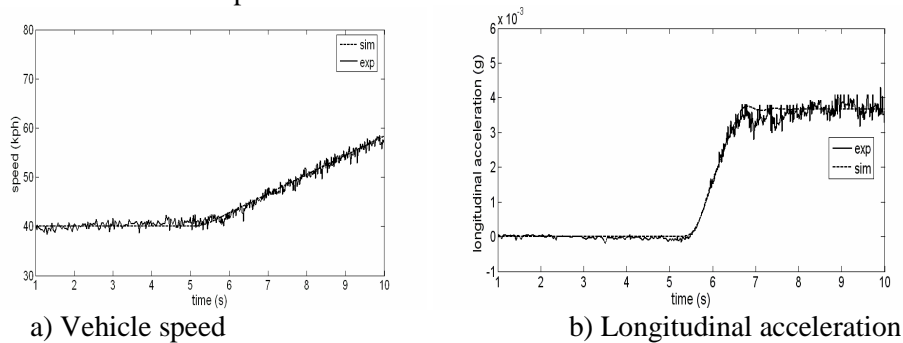
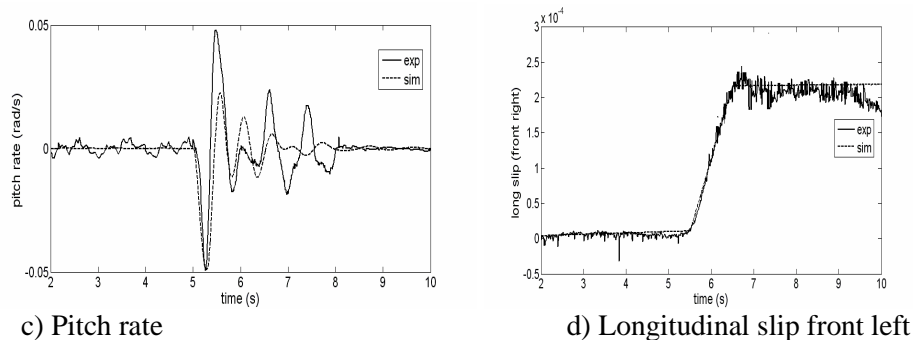
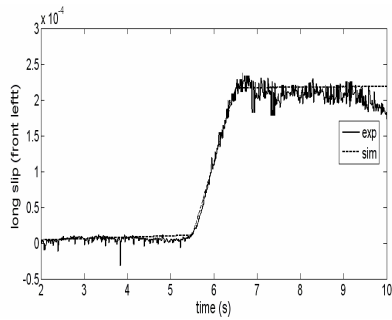
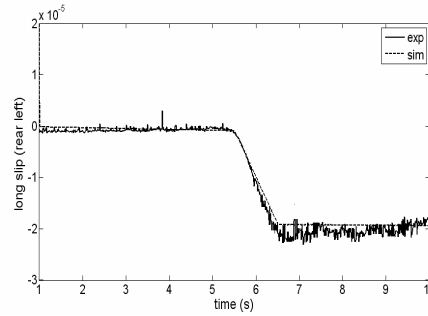


Figure 9: Response of the vehicle for sudden acceleration test at constant speed 40kph

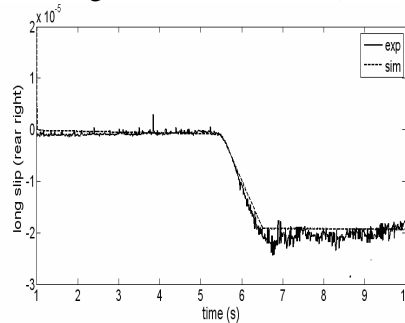




e) Longitudinal slip front right



f) Longitudinal slip rear left



g) Longitudinal slip rear right

Figure 10 : Continue

Overall, it can be concluded that the trends between simulation results and experimental data are having good agreement with acceptable error. Actually, the error can be significantly reduced by fine tuning of both vehicle and tire parameters. However, excessive fine tuning works can be avoided since in control oriented model, the most important characteristic is the trend of the model response. As long as the trend of the model response is closely similar with the measured response with acceptable deviation in magnitude, it can be said that the model is valid.

5.0 PERFORMANCE ASSESSMENT OF THE PROPOSED CONTROL STRUCTURE FOR ACTIVE SUSPENSION SYSTEM

This section describes the results of study on the performance of the proposed control structure for the pneumatically actuated active suspension system namely PID with pitch moment rejection control. Performance of the vehicle with passive system is used as a basic benchmark. To investigate the advantage of additional pitch moment rejection loop, the performance of the proposed controller is also compared with PID without pitch moment rejection loop. The PID with pitch moment rejection control for active suspension system is evaluated for its performance at controlling the longitudinal dynamics of the vehicle according to the following performance criteria namely body vertical acceleration, body displacement, body pitch rate and body pitch angle.

5.1 Simulation Parameters

The simulation study was performed for a period of 10 seconds using Heun solver with a fixed step size of 0.01 second. The controller parameters are obtained using trial and error technique as shown in Table 3. The numerical values of the 14-DOF full vehicle model parameters are defined in Table 1 and Calspan tire model parameters are as Table 2 adopted from Szostak *et al.* [36].

Table 2: Tire parameter

Parameter	FWD radial
Tire designation	P185/70R13
T_w	7.3
T_p	24
F_{ZT}	980
C_1	1.0
C_2	0.34
C_3	0.57
C_4	0.32
A_o	1068
A_1	11.3
A_2	2442.73
A_3	0.31
A_4	-1877
K_a	0.05
CS/FZ	17.91
μ_o	0.85

Table 3: Controller Parameters:

PID	k_p	k_i	k_d
body heave (Zb)	2000	2000	3000
body pitch angle (θ)	1852	7000	2251

5.2 Performance of The Control Structure At The Sudden Braking Test

The simulation results of body pitch angle and body pitch rate at the body centre of gravity on sudden braking test at 6Mpa brake pressure are shown in Figures 11(a) and (b) respectively. It can be seen that the performance of PID control with pitch moment rejection loop are perfectly can normalized the body compare to PID control without pitch moment rejection loop and passive system. In terms of the pitch angle response, it is clear that the additional pitch moment rejection loop can effectively reduce the magnitude of the pitch angle response. Improvement in pitch motion during braking can enhance the stability of the vehicle in longitudinal direction.

In terms of the pitch rate response, PID control with pitch moment rejection loop shows significant improvement over passive and PID control without pitch

moment rejection loop particularly in the transient response area. In steady state response, PID control with pitch moment rejection loop shows slight improvement in terms of settling time over PID control without pitch moment rejection loop and significant improvement over passive system. Again, the advantage of the additional pitch moment rejection loop is shown by reducing the magnitude of the pitch rate response. Improvement in both pitch rate response and the settling time during maneuvering can increase the stability level of the vehicle in the presence of braking input from the driver.

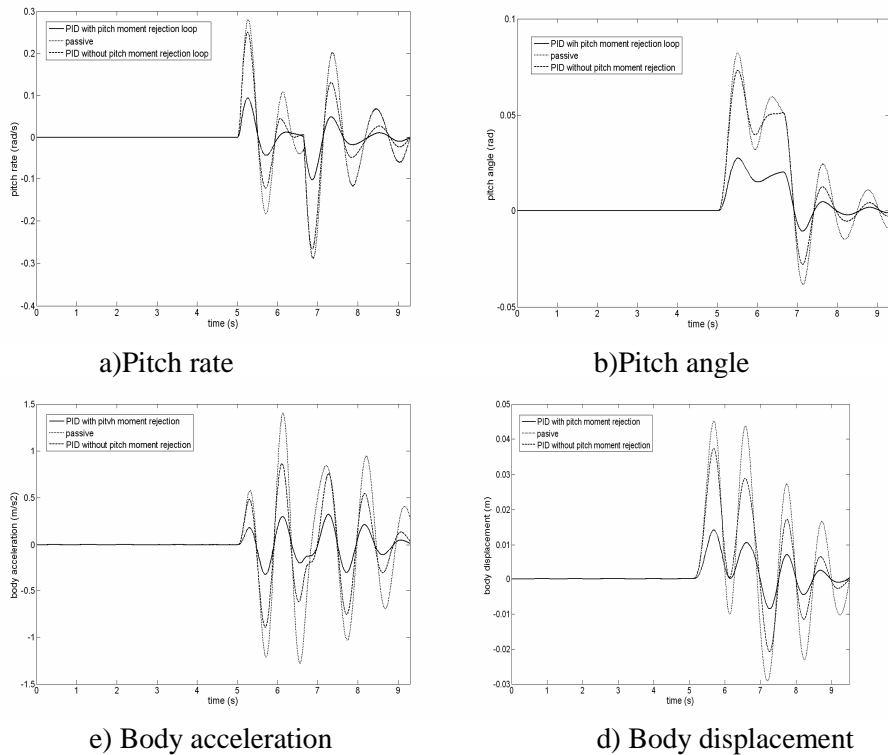


Figure 11: Response of the vehicle for sudden braking test at 6Mpa brake pressure.

Body vertical acceleration responses of the vehicle at the body center of gravity are presented in Figure 11(c). From the body vertical acceleration response, both PID control with and without pitch moment rejection loops are able to drastically reduce unwanted vertical acceleration compared to the passive system. It can be seen by the capability of the controller in lowering down the magnitude of body acceleration and in speeding up the settling time. Improvement in vertical acceleration at the body center of gravity will enhance the comfort level of the vehicle as well as avoiding the driver from losing control of the vehicle during maneuvering. The PTP and RMS values of pitch angle, body acceleration, body displacement and pitch rate on sudden braking test is presented in Table 3.

Table 4: PTP and RMS values of simulation for sudden braking test at 6mpa brake pressure

Performance Criteria	PTP Value			RMS Value		
	passive	PID without pitch moment rejection	PID with pitch moment rejection	passive	PID without pitch moment rejection	PID with pitch moment rejection
Pitch Angle	0.129	0.121	0.06	0.0232	0.0198	0.0077
Pitch Rate	0.59	0.55	0.19	0.1191	0.0938	0.0361
Body Acceleration	2.81	1.771	0.487	0.6263	0.3882	0.161
Body Displacement	0.0776	0.0571	0.0232	0.0196	0.0127	0.0051

5.3 Performance of The Control Structure At The Sudden Acceleration Test

Figure 18 shows the simulation result of the vehicle under the PID active suspension control with pitch moment rejection loop, PID control without pitch moment rejection loop, and passive suspension system for comparison purposes. The result shows that the PID controller with moment rejection loop has good performance in tracking of system and also the system is stable and has good transient response. Consider to Figures 12(a) and (b), the pitch behavior for the PID control with pitch moment rejection loop indicate better performance reduce squat during the maneuver compared to PID without pitch moment rejection loop and passive. The results show that the proposed control structure is reasonably efficient method to decrease the vehicle pitch rate. As a result vehicle loses the momentum during the maneuvers, reduce the weight transfer to the front and decrease the pitch angle magnitude at body center of gravity.

Figure 12(c) illustrates clearly how the PID control with pitch moment rejection loop can effectively absorb the vehicle vibration in comparison to PID without pitch moment rejection loop and the passive system. The oscillation of the body acceleration using the PID with pitch moment rejection loop system is very much reduced significantly, which guarantees better ride comfort and reduced the body vertical displacement as shown in Figure 12(d). In steady state response, PID control with pitch moment rejection loop shows slight improvement in terms of settling time over PID control without pitch moment rejection loop and significant improvement over passive system. Improvement in both body acceleration response and the settling time during maneuvering can increase the stability level of the vehicle in the presence of throttle input from the driver. The PTP and RMS values of pitch angle, body acceleration, body displacement and pitch rate on sudden acceleration test is presented in Table 4.

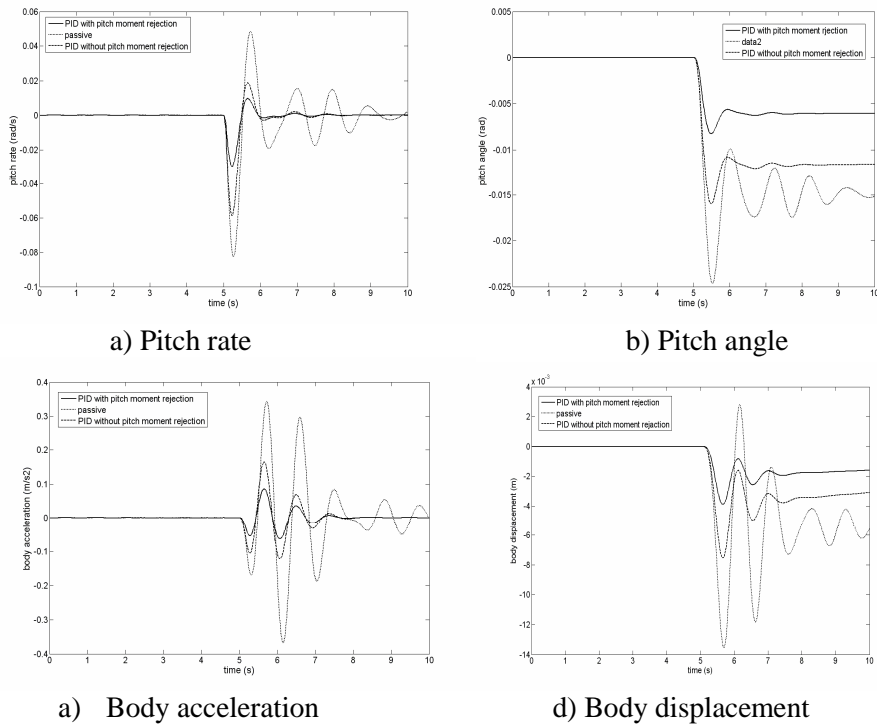


Figure 12: Response of the vehicle for sudden acceleration test at full step throttle pedal

Table 5: PTP and RMS values of simulation results for sudden acceleration test at full step throttle

Performance Criteria	PTP Value			RMS Value		
	passive	PID without pitch moment rejection	PID with pitch moment rejection	passive	PID without pitch moment rejection	PID with pitch moment rejection
Pitch Angle	0.0248	0.0167	0.0074	0.0114	0.0088	0.0045
Pitch Rate	0.13	0.08	0.03	0.0191	0.0112	0.0058
Body Acceleration	0.767	0.27	0.088	0.1104	0.0415	0.0214
Body Displacement	0.0168	0.008	0.00389	0.0048	0.0028	0.0015

6.0 CONCLUSIONS

A 14-DOF full vehicle model for passenger vehicle which consists of ride, handling and Calspan tire subsystems has been developed. The models are verified with CarSimEd software as the benchmark to observe the performance and the capability of the vehicle model to perform the validation with experimental vehicle. Predictions of the results show that the model are satisfying similarity with only small deviation compare to the software and accepted for the validation with experimental vehicle. An instrumented experimental vehicle has been developed to validate the 14-DOF model with the necessary sensors and data acquisition system installed inside the vehicle. Two types of road tests namely sudden braking test and sudden acceleration test have been performed and data gathered from the tests were used as the benchmark of the model validation. The wheel speed data measured from the test in both sudden braking and sudden acceleration tests were used as the inputs of the simulation model. Some of the vehicle behaviors to be validated in this works were pitch rate, longitudinal acceleration and tire longitudinal slip responses. The results of model validation show that the trends between simulation results and experimental data are almost similar with acceptable error. The small difference in magnitude between simulation and experimental results is mainly due to the simplification/idealization in vehicle dynamics modeling and the difficulty of the driver to maintain a constant speed during maneuvering.

On the other hand a PID controller with pitch moment rejection loop is presented to reduce unwanted vehicle motion in longitudinal direction for enhance vehicle stability and ride quality. A simulation studies for proposed control structure with validated full vehicle model are presented to demonstrate the effectiveness of pitch moment rejection loop combined with PID control. The performance characteristics of the control structure are evaluated and compared with PID control without pitch moment rejection loop and passive system. From the results, it can be concluded that the proposed control technique proved to be effective in controlling vehicle pitch, vibration and achieve better performance. The controller is also verified able to enhance the vehicle stability and ride quality as the improvement in body acceleration in the simulation responses.

ACKNOWLEDGEMENT

This work is supported by the Ministry of Science Technology and Innovation (MOSTI) through it scholarship and financial support and Ministry of Higher Education (MoHE) of Malaysia through FRGS project entitled "Development of a Pneumatically Actuated Active Stabilizer Bar to Reduce Unwanted Motion In Longitudinal Direction" lead by Dr. Khisbullah Hudha at the Universiti Teknikal Malaysia Melaka. This financial support is gratefully acknowledged.

REFERENCES

1. Fenchea, M. 2008. Influence of Car's Suspension in the Vehicle Comfort and Active Safety. *Annals of the University of Oradea, Fascicle of Management and Technology Engineering*. Vol. VII (XVII).
2. Ahmad, F., Hudha, K., Said. M. R. and Rivai. A. 2008a. Development of Pneumatically Actuated Active Stabilizer Bar to Reduce Vehicle Dive. *Proceedings of the International Conference Plan Equipment and Reliability*. March 27-28. Kuala Lumpur, Malaysia
3. Ahmad, F., Hudha, K., Said. M. R. and Rivai. A. 2008b. Development of Pneumatically Actuated Active Stabilizer Bar To Reduce Vehicle squat. *Proceedings of the 3rd Brunei International Conference on Engineering and Technology 2008*. November 2-5. Bandar Sri Begawan, Brunei Darussalam
4. Bahouth, G. 2005. Real World Crash Evaluation of Vehicle Stability Control (VSC) Technology. *49th Annual Proceedings Association for the Advancement of Automotive Medicine*.
5. Weeks, D. A., Beno, J. H., Guenin, A. M. and Breise, D. A. 2000. Electromechanical Active Suspension Demonstration for Off Road Vehicles. *SAE Technical Paper Series*. Vol.01, No.0102.
6. Md. Sam, Y. and Osman, and Shah, J. H. 2006. Sliding Mode Control of a Hydraulically Actuated Active Suspension. *Jurnal Teknologi, Universiti Teknologi Malaysia*. Vol.3, No.44, pp.37-48
7. Gao, B., Darling, J., Tilley, D. G. and Williams, R.A. 2006. Modeling and Simulation of a Semi-active Suspension System. *Department of Mechanical Engineering, University of Bath, Bath a.d Engineering Centre, Jaguar and Land Rover, Whitely, Coventry, BA2 7AY, CV3 4LF*.
8. Sampson, D.J.M., Jeppesen, B.P. and Cebon, D. 2000. The Development of an active roll control system for heavy vehicles. *In Proceedings of 6th International Symposium on Heavy Vehicle Weights and Dimensions*. pp. 375–384.
9. Hudha, K., Jamaluddin, H. Samin, P. M. and Rahman, R. A. 2003. Semi Active Roll Control Suspension System on a New Modified Half Car Model. *SAE Technical Paper Series*. Paper No. 2003-01-2274.
10. Toshio, Y. and Itaru, T. 2005. Active Suspension Control of a One-wheel Car Model Using Single Input Rules Modules Fuzzy Reasoning and a Disturbance Observer. *Journal of Zheijiang University SCIENCE*. Vol.6A, No. 4, pp. 251-256.
11. March, C. and Shim, T. 2007. Integrated Control of Suspension and Front Steering to Enhance Vehicle Handling. *Proc. IMEche. Journal of Automobile Engineering*. vol. 221, No. 152, pp, 377-391.
12. Mailah, M. and Priyandoko, G. 2007. Simulation of a Suspension System with Adaptive Fuzzy Active Force Control. *International Journal of Simulation Modeling*. 6 (1). pp. 25-36. ISSN 1726-4529
13. Wang, F.C. and Smith, M.C. 2002. Active and Passive Suspension Control for Vehicle Dive and Squat. *In: Johansson, R. and Rantzer, A., (eds.)*

- Nonlinear and Hybrid Systems in Automotive Control. Springer-Verlag. London, UK. pp. 23-39. ISBN 1852336528*
14. Labaryade, R. and Aubert, D. 2003. A Single Framework for Vehicle Roll, Pitch, Yaw Estimation and Obstacles Detection by Stereovision. *Proceedings IEEE on Intelligent Vehicles Symposium. June 9-11. Columbus, USA. pp. 31-36.*
 15. Kruczek, A. and Stribrsky, A. 2004. A Full-car Model for Active Suspension – Some Practical Aspects’, *Proceedings of the IEEE International Conference on Mechatronics. June 3-5. Istanbul Turkey. pp. 41-45.*
 16. Toshio, Y. and Atsushi, T. 2004. Pneumatic Active Suspension System for a One-Wheel Car Model Using Fuzzy Reasoning and a Disturbance Observer. *Journal of Zhejiang University SCIENCE. Vol. 5, No. 9, pp. 1060-1068.*
 17. Campos, J., Davis, L., Lewis, F., Ikanega, S., Scully, S. and Evans, M. 1999. Active suspension system control of ground vehicle heave and pitch motions. *Proceedings of the 7th IEEE Mediterranean Control Conference on Control and Automation. June 28-30.*
 18. Vaughan, J., Singhose, W. and Sadegh, N. 2003. Use of Active Suspension Control to Counter the Effects of Vehicle Payloads. *Proceeding of IEEE Conference on Control Applications, 2003 Istanbul, (CCA 2003). June 23-25. Istanbul, Turkey. Vol. 1 pp. 285-289*
 19. Ikanega, S. and Lewis, F. L., Campos, J. and Davis, L. 2000. Active Suspension Control of Ground Vehicle Based on a Full-Vehicle Model. *Proceeding of the American Control Conference on Ground Vehicle Based. Chicago, June, Illinois, USA. June 28-30*
 20. Zhang, Y., Zhao, L., Cong, H. and Wang, B. 2004. Study on Control of Vehicle Attitude and Ride Comfort Based on Full-car Model. *Fifth World Congress on Intelligent Control and Automation, 2004. (WCICA 2004). Vol.4, pp. 3514- 3519.*
 21. Donahue, M. D. 2001. Implementation Of An Active Suspension, Preview Controller For Improve Ride Comfort. *Master Thesis University of California, Berkeley.*
 22. Sampson, D.J.M. and Cebon, D. 2003a. Achievable Roll Stability of Heavy Road Vehicles. *Proc. Instn Mech. Engrs, Part : J. Automobile Engineering. 217(4), pp. 269–287.*
 23. Sampson.D.J.M and Cebon.D. 2003b. *Active Roll Control of Single Unit Heavy Road Vehicles. Vehicle System Dynamics, International Journal of Vehicle Mechanics and Mobility. Vol. 40, Issue. 4. pp. 229–270.*
 24. Karnopp, D. 1995. Active and Semi-active Vibration Isolation. *Journal of Mechanical Design, ASME. Vol.177, pp. 177-185.*
 25. Yoshimura, T., Isari, Y., Li, Q. and Hino, J. 1997a. Active Suspension of Motor Coaches Using Skyhook Damper and Fuzzy Logic Controls. *Control Engineering Practice. Vol. 5, No. 2, pp. 175-184.*
 26. Yoshimura, T., Nakaminami, K. and Hino, J. 1997b. A Semi-active Suspension with Dynamic Absorbers of Ground Vehicles Using Fuzzy Reasoning. *International Journal of Vehicle Design, Vol. 18, No. 1, pp. 19-34.*
 27. Yoshimura, T., Hiwa, T., Kurimoto, M. and Hino, J. 2003. Active Suspension of a One-wheel Car Model Using Fuzzy Reasoning and

- Compensators. *International Journal of Vehicle Autonomous Systems*, Vol. 1, No. 2, pp. 196-205.
28. Yoshimura, T. and Watanabe, K. 2003. Active Suspension of a Full Car Model Using Fuzzy Reasoning Based on Single Input Rule Modules with Dynamic Absorbers', *International Journal of Vehicle Design*, Vol. 31, No. 1, pp. 22-40.
 29. Yoshimura, T., Kume, A., Kurimoto, M. and Hino, J. 2001. Construction of An Active Suspension System of a Quarter Car Model Using the Concept of Sliding Mode Control. *Journal of Sound and Vibration*, Vol. 239, No. 2, pp. 187-199
 30. Stilwell, D. J. and Rugh, W. J. 1999. Interpolation of Observer State Feedback Controllers for Gain Scheduling. *IEEE Transactions on Automatic Control*. Vol. 44, No. 6, pp. 1225-1229.
 31. Lee, C. H., Shin, M. H. and Chung, N. J. 2001. A Design of Gain-Scheduled Control for a Linear Parameter Varying System: An Application to Flight Control. *Control Engineering Practice* 9, pp. 11-21
 32. Sedaghati, A. 2006. A PI Controller Based on Gain-Scheduling for Synchronous Generator. *Turkish Journal of Electrical Engineering and Computer Sciences*. Vol.14, No.2.
 33. Fialho, I and Balas, G. J. 2002. Road Adaptive Active suspension Design Using Linear Parameter Varying Gain-Scheduling. *IEEE Transactions on Control System Technology*. Vol. 10, No. 1, pp. 43-51.
 34. Kadir, Z. A., Hudha, K., Nasir, M. Z. M. and Said, M. R. 2008. Assessment of Tire Models for Vehicle Dynamics Analysis. *Proceedings of the International Conference on Plant Equipment and Reliability*. March 27-28. Kuala Lumpur, Malaysia.
 35. Ahmad, F., Hudha, K. Rivai. A. and Zakaria, M. M. N. 2008c. Modeling And Validation of Vehicle Dynamic Performance in Longitudinal Direction. *Submitted to Journal Of Advanced Manufacturing (JAMT)*.
 36. Szostak, H. T., Allen, W. R. and Rosenthal, T. J. 1988. Analytical Modeling of Driver Response in Crash Avoidance Maneuvering Volume II: An Interactive Model for Driver/Vehicle Simulation. *US Department of Transportation Report NHTSA DOT HS-807-271*. April.
 37. Singh, T., Kesavadas, T., Mayne, R., Kim, J. J. and Roy, A. 2002. Design of Hardware/Algorithms for Enhancement of Driver-vehicle Performance in Inclement Weather Conditions Using a Virtual Environment. *SAE 2004 Transactions Journal of Passenger Car: Mechanical Systems*. Paper No. 2002-01-0322.